

Isotactic Polypropylene. Unperturbed Dimensions Calculated Accounting for All Skeletal Rotations

G. Allegra,*^{1a} M. Calligaris,^{1a} L. Randaccio,^{1a} and G. Moraglio^{1b}

Istituto di Chimica, Università di Trieste, 34127 Trieste, Italy, and the Istituto di Chimica Industriale del Politecnico, 20133 Milan, Italy. Received May 11, 1972

ABSTRACT: The algorithm described in a preceding paper for the statistical mechanical treatment of ...A-B-A-B... chains with neighbor interactions is applied to isotactic polypropylene. It allows accounting for all possible skeletal rotations (asr scheme), in contrast with the usual method based on the rotational isomeric state approximation (ris scheme). The unperturbed mean-square end-to-end distance as well as its temperature coefficient are calculated using two distinct sets of non-bonded interaction parameters. Within the asr scheme the results for either set may be put in good agreement with the experimental data by adopting a reasonable value of the van der Waals radius of the methyl group. Assumption of steric defects is therefore unnecessary. The ris scheme is not easily applicable using the same energy maps because of the strong correlation between neighboring rotation angles, which makes the choice of the rotational isomers subjected to some uncertainty. The chain conformational energy at various temperatures is also calculated: the intramolecular contribution, which is about 20% of the heat of melting, has approximately the same value whichever method (*i.e.*, asr or ris) is applied.

General Comparison between the Rotational Isomeric State Approach and That Considering All the Skeletal Rotations. The rotational isomeric state (ris) approach has proved to be considerably powerful in explaining the unperturbed dimensions derived from experiment for many polymers.^{1c,2} However, it seemed to fail in the case of isotactic polypropylene (IPP) until recent calculations appeared in the literature,³ since, no matter what parameters were chosen for the interaction potentials between non-bonded atoms, the calculated characteristic ratio ($C_\infty = \langle r^2 \rangle_0 / 2Nl^2$, N and l being the number of monomer units and the C-C bond length, respectively) was invariably much larger⁴⁻⁶ than the experimental figure.^{7,8} Moreover, at least until recent experimental data^{8,9} and theoretical results³ became available, the (negative) calculated temperature derivative of C_∞ appeared to be invariably too large in comparison with experiment. Lately, Boyd and Breitling tackled the configurational problem of IPP within the ris scheme starting from least-squares energy calculations, with several geometrical parameters allowed to participate.³ They were able to obtain a reasonable agreement between calculations and the most reliable experimental data.

In a systematic attempt to assess the relative merits of the ris scheme and of the approach which takes into account the whole spectrum of skeletal rotations (all skeletal rotations, or asr scheme),^{10,11} we have applied to IPP the latter method of calculation. The inherent limitations of the asr scheme are¹¹: (i) the current approximation of classical statistical mechanics that the molecular parti-

tion function may be factorized into a configurational and a kinetic component; (ii) the need to obtain essentially correct energy maps; (iii) the assumption that energy correlation is confined to first-neighboring rotations (no doubt longer range interactions might also be accounted for, but at the expense of much trickier computations).

A simpler mathematical formulation and an easier connection with physical intuition are the main advantages of the ris scheme. As for the above points, it suffers from assumption i as well, at least until a clear physical meaning is to be attributed to the current conformational energy calculations. The same consideration also applies to assumption ii. However, within the ris scheme the various uncertainties associated with the calculated energy maps are easily accounted for through the adjustment of some statistical weights in order to fit the experimental data (see, *e.g.*, ref 2, chapters V and VI). The logical counterpart, in the asr scheme, may be represented by the introduction of some adjustable parameters into the energy potentials between non-bonded atoms (*cf.* the variable radius of the methyl group, see following). It should be clear, though, that in either case this is obtained at the expense of some logical consistency. As for problem iii, this is more easily circumvented in the ris scheme, but is rarely needed. In addition—and this appears to be the most serious drawback of the ris approach, in principle—the neglect of all the conformations which do not correspond to true energy minima may lead to serious loss of accuracy. Suppose, for instance, that a given minimum is substantially elongated in the direction of one (or more) rotation angle. In the ris scheme this is usually accounted for with the introduction of some factor which multiplies the statistical weight $\exp(-E/RT)$ corresponding to the minimum energy, in order to account for the entropy contribution related with the size of the minimum. But the angular functions—sines and cosines of the angles appearing in the rotation matrices—should also so modified, *i.e.*, averaged over the whole area of the minimum. A more complicated situation (and we shall see that it happens just in the case of IPP) corresponds to having minima which are stretched along some diagonal direction in the energy map relating two neighboring rotation angles (*i.e.*, φ_i and φ_{i+1} , i being the index of the chain skeletal bond). In this case, it seems difficult to escape the conclusion that the ris scheme should be applied after splitting the minimum into two or more minima properly displaced along the direction of elongation.

- (1) (a) Università di Trieste; (b) Istituto di Chimica Industriale del Politecnico; (c) T. M. Birshtein and O. B. Ptitsyn in "Conformations of Macromolecules," Translated from the 1964 Russian Edition, S. N. Timasheff and M. J. Timasheff, Ed., Interscience, New York, N. Y., 1966.
- (2) P. J. Flory, "Statistical Mechanics of Chain Molecules," Interscience, New York, N. Y., 1969, Chapter V.
- (3) R. H. Boyd and S. M. Breitling, (a) *Polym. Prepr., Amer. Chem. Soc. Div. Polym. Chem.*, 13, 342 (1972); (b) *Macromolecules*, 5, 279 (1972).
- (4) (a) P. Corradini and G. Allegra, *Atti Accad. Naz. Lincei, Cl. Sci. Fis. Mat. Natur., Rend.*, 30, 516 (1961); (b) G. Allegra, P. Ganis, and P. Corradini, *Makromol. Chem.*, 61, 225 (1963).
- (5) T. M. Birshtein and O. B. Ptitsyn, *Zh. Tekh. Fiz.*, 29, 1075 (1959).
- (6) P. J. Flory, J. E. Mark, and A. Abe, *J. Amer. Chem. Soc.*, 88, 639 (1966).
- (7) (a) J. B. Kinsinger and R. E. Hughes, *J. Phys. Chem.*, 63, 2002 (1959); (b) J. B. Kinsinger and R. E. Hughes, *ibid.*, 67, 1922 (1963).
- (8) A. Nakajima and A. Sayji, *J. Polym. Sci., Part A-2*, 6, 735 (1968).
- (9) G. Moraglio *et al.*, unpublished results.
- (10) G. Allegra and A. Immirzi, *Makromol. Chem.*, 124, 70 (1969).
- (11) G. Allegra, M. Calligaris, and L. Randaccio, *Macromolecules*, 6, 390 (1973).

Table I
Parameters for the Non-bonded Interactions ($V_{ab} = A_{ab} \exp(-C_{ab}r_{ab})/r_{ab}^n - B_{ab}^6$)^a

$r(\text{CH}_3)$ (Å) ^b	Set I					Set II			
	A_{ab}	B_{ab}	C_{ab}	n		A_{ab}	B_{ab}	C_{ab}	n
C...C	2.94×10^5	381	0	12		2.53×10^5	327	0	12
C...H	3.97×10^4	134	0	12		2.33×10^4	125	2.04	6
H...H	4.71×10^3	49	0	12		2.82×10^3	49	4.08	0
CH ₃ ...CH ₃	2.00	5.64×10^6	2750	0	12	1.96×10^5	2942	3.33	0
	1.90	4.14×10^5	2750	0	12	1.45×10^5	2942	3.33	0
	1.85	3.53×10^6	2750	0	12				
	1.80	3.00×10^6	2750	0	12	1.08×10^5	2942	3.33	0
	1.70	2.94×10^6	2750	0	12	0.83×10^5	2942	3.33	0
H...CH ₃	2.00	1.63×10^5	367	0	12	2.53×10^4	380	3.71	0
	1.90	1.40×10^5	367	0	12	2.18×10^4	380	3.71	0
	1.85	1.29×10^5	367	0	12				
	1.80	1.19×10^5	367	0	12	1.89×10^4	380	3.71	0
	1.70	1.02×10^5	367	0	12	1.66×10^4	380	3.71	0
C...CH ₃	2.00	1.29×10^6	1024	0	12	2.29×10^5	981	1.67	0
	1.90	1.10×10^6	1024	0	12	1.97×10^5	981	1.67	0
	1.85	1.02×10^6	1024	0	12				
	1.80	0.94×10^6	1024	0	12	1.69×10^5	981	1.67	0
	1.70	0.79×10^6	1024	0	12	1.45×10^5	981	1.67	0

^a r_{ab} in Å; V_{ab} in kcal/mol. ^b The van der Waals radii of C and H are 1.70 and 1.20 Å, respectively.

In this connection, we wish to point out another logical difficulty which may be encountered within the ris scheme, with no counterpart in the asr scheme. Suppose the energy maps $E(\varphi_i\varphi_{i+1})$ and $E(\varphi_{i+1}\varphi_{i+2})$ are being considered. Since the assumption of first-neighbor correlation is done, no map depending on more than two angles need be calculated. In the ris scheme, definition of the minimum energy angles is required, but the values corresponding to φ_{i+1} may not be the same in the first and in the second map. The difficulty may seem to be circumvented by considering the minimum energy values of the function $E(\varphi_i\varphi_{i+1}) + E(\varphi_{i+1}\varphi_{i+2})$, except that the same problem now applies to φ_i and to φ_{i+2} , and so on. In other words, if the rotational isomers must correspond to conformations with a stationary energy, as is currently assumed, the existence of energy correlation through all the rotation angles of the chain should be considered even though the separate energy terms apply to neighboring pairs. The problem can be easily solved if, around a given local minimum, each energy contribution $E(\varphi_i\varphi_{i+1})$ may be split into a sum of the type $E(\varphi_i) + E(\varphi_{i+1})$, which allows the energy minimization to be carried out along each rotation angle separately. Since this happens very frequently in practice, the above problem has rarely represented a serious hindrance to ris calculations, especially if the several sources of uncertainty related with the energy maps are also taken into consideration. However, as will be stressed in the following, the existence of this correlation effect plays a significant role in the case of IPP. At least partial evidence of the real existence of this effect may be recognized in the results obtained by Boyd and Breitling for the geometries of the conformational isomers of 2,4,6-trimethylheptane. With reference to Table II of ref 3b, the sequence TT-G'-G'TG, e.g., cannot be exactly described in the polymer as resulting from the two interlocking sequences (TT-G'-G') and (G'-G'TG) of the model compound, since the two rotations in common (i.e., G'- and G') differ by as much as 15° in the two conformers. However, it must be added that this source of inaccuracy has probably very little effect in Boyd and Breitling's treatment.

As a final comment, there appears to be now a reason-

able hope that new methods of computation will allow in the near future to obtain more and more accurate energy maps, which will take advantage eventually of the progress of quantum mechanics in the computation field. As for the time being, energy optimization over several structural parameters (especially over bond angles, in addition to rotation angles^{3,12}) already leads to significant improvement in the calculation of conformational energy maps for polymers, even without recourse to quantum mechanics.

Conformational Energy Maps. In our conformational calculations we have assumed the methyl group as a spherically symmetrical body, taking its van der Waals radius ($r(\text{CH}_3)$) as an adjustable parameter in the range 1.7–2 Å, i.e., less than the usually accepted figure (2 Å¹³). We have verified that the value which fits at best the experimental data is close to that producing the experimental gauche-trans energy difference of *n*-butane (0.8 kcal/mol¹⁴).

In order to justify these assumptions, let us point out that the non-bonded interactions involving methyl groups are influenced to a large extent by several, although restricted, degrees of freedom corresponding to rigid rotation around the C-CH₃ bonds as well as to elastic bending of bond angles. As a first consequence, unless a very elaborate procedure is followed where all these parameters are allowed to vary, the detailed consideration of all the H...H, H...C, and C...C interactions is better given by a potential function depending on the C...X distance only.¹² Furthermore, if the coefficient of the attractive component of the potential (i.e., the coefficient of r^{-6}) is calculated according to the Slater-Kirkwood approximation¹⁵ assuming an effective electron number in proportion with the size of the CH₃ group (i.e., larger than 20), the calculated CH₃...X interactions at short intergroup distance are exceedingly large. Again this is due to the (rotational + bending) flexibility, which makes

- (12) G. Allegra, E. Benedetti, C. Pedone, *Macromolecules*, **3**, 727 (1970).
- (13) L. Pauling, "The Nature of the Chemical Bond," Cornell University Press, Ithaca, N. Y., 1960, p 260.
- (14) G. J. Szasz, N. Sheppard, and D. H. Rank, *J. Chem. Phys.*, **16**, 704 (1948).
- (15) K. S. Pitzer, *Advan. Chem. Phys.*, **2**, 59 (1959).

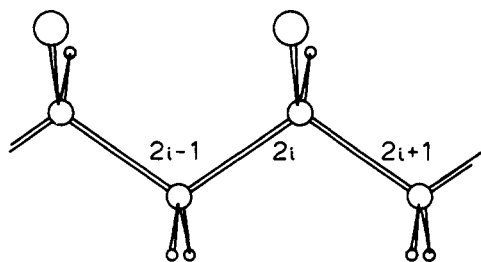


Figure 1. A sketch of the isotactic polypropylene chain in an arbitrary zigzag planar conformation.

the methyl group "softer" than expected for a normal atom with a similar size and justifies the assumption of $r(\text{CH}_3)$ as a free parameter.

Since uncertainty in the non-bonded interaction functions is a major cause of error in the semiempirical conformational analysis of the present type, we have employed two different sets of data (see Table I). The first set (set I) has already been used by one of us for the conformational analysis of poly(isobutylene)¹² and is basically similar to that proposed by Scott and Scheraga¹⁶ with the addition of the parameters involving the methyl group which have been calculated with an effective number of electrons equal to 22. The other set (set II) was proposed by Giglio after an analysis of the crystalline packing of some organic compounds.¹⁷ Here the effective number of electrons attributed to the methyl group is about 19, which means that the corresponding non-bonded interaction potentials at short distances are softer than the previous ones (*i.e.*, they involve a smoother change of energy with interatomic distance). As we shall see, the experimental data are explained reasonably well with rather similar values of $r(\text{CH}_3)$ in either set.

The general procedure of calculation is closely parallel to that followed by some of us for poly(oxyethylene).¹¹ Referring to Figure 1 for the labeling of the skeletal bonds, there are two nonequivalent pairs of neighboring rotations per monomer unit, namely, $(\varphi_{2i-1}\varphi_{2i})$ and $(\varphi_{2i}\varphi_{2i+1})$. For each pair the potential energy function has been evaluated as

$$E(\varphi_n\varphi_{n+1}) = \frac{1}{2}U_0(1 + \cos 3\varphi_n) + \sum_{i < j} V_{ij}(r_{ij}) \quad (1)$$

where U_0 is the inherent threefold barrier to the rotation around C-C bonds, and V_{ij} is the non-bonded interaction energy between the atoms or groups labeled as i and j , as a function of their distance r_{ij} . We have put $U_0 = 3$ kcal/mol, as in ethane.¹⁸ The non-bonded distances are only a function of the rotation angles, since both the bond lengths and the angles have been kept fixed ($l_{\text{C-C}} = 1.54$ Å; $l_{\text{C-H}} = 1.08$ Å; bond angles tetrahedral). Since no interaction between atoms separated by more than four bonds may be specified by two rotation angles only, for either plot we have calculated the V_{ij} term between skeletal atoms separated by four bonds (*i.e.*, two methylenic carbons in the odd-even and two tertiary carbons in the even-odd plot) as formally due to methyl groups, in order to account approximately for the steric effect of their surrounding hydrogen atoms.

Calculations have been carried out for both sets of non-bonded interaction parameters with $[r(\text{CH}_3)] = 1.70, 1.80, 1.90$, and 2.00 Å. For set I $r(\text{CH}_3) = 1.85$ Å has also been considered (see Table I for the list of the parameters). For

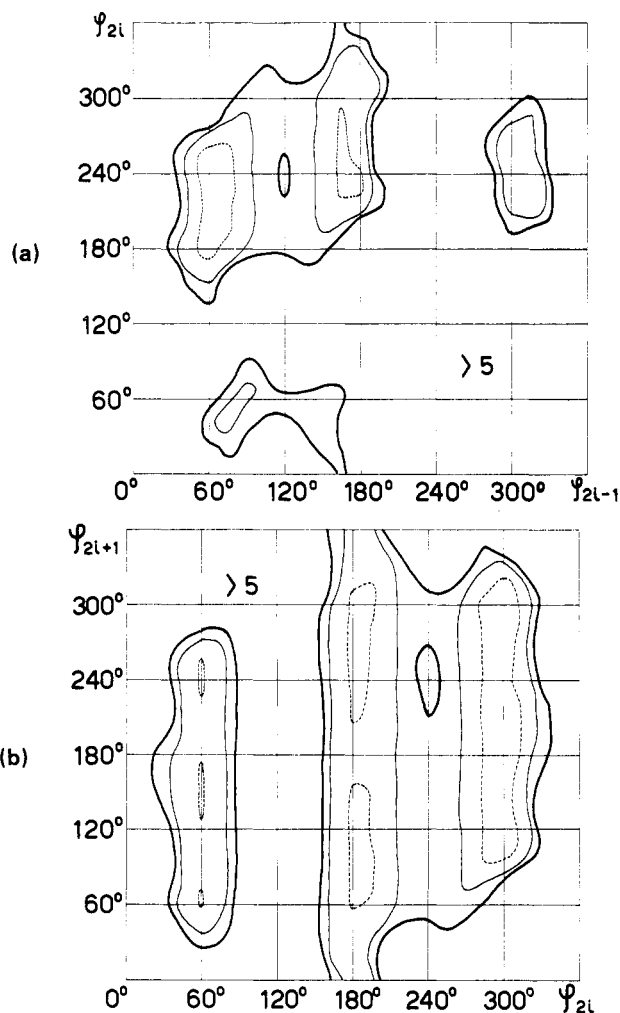


Figure 2. $E(\varphi_{2i-1}\varphi_{2i})$ (a) and $E(\varphi_{2i}\varphi_{2i+1})$ (b) plots (see Figure 1). Energy levels are drawn at 1 (dashed line), 3.5 (heavy line) kcal/mol.

each set the B (attractive) coefficient of the potential between a methyl group CH_3 and any other atom X has been calculated as the geometrical average $(B(\text{CH}_3\text{-CH}_3) \cdot B(X\text{-}X))^{1/2}$, which the A (repulsive) coefficient has been given the value which determines the minimum of the function in correspondence to the sum of the van der Waals radii. As an example, in Figure 2 the conformational energy plots corresponding to set I and $r(\text{CH}_3) = 1.80$ Å are shown. As a particular illustration of the use of the diagrams, the energy per monomer unit corresponding to a regular helical conformation of the chain (E_h) may be obtained as follows.¹¹ According to the equivalence postulate¹⁹ all the monomer units have the same conformation, which means that φ_{2i-1} 's have the same value (φ_I), as well as all φ_{2i} 's (φ_{II}), for any index i . Therefore $E_h(\varphi_I\varphi_{II})$ is given by

$$\begin{aligned} E_h(\varphi_I\varphi_{II}) &= E(\varphi_{2i-1}\varphi_{2i}) + E(\varphi_{2i}\varphi_{2i+1}) \\ \varphi_{2i-1} &= \varphi_{2i+1} = \varphi_I \\ \varphi_{2i} &= \varphi_{II} \end{aligned} \quad (2)$$

Figure 3 shows the plot of $E_h(\varphi_I\varphi_{II})$, which is very similar to other intramolecular energy maps previously obtained

(16) R. A. Scott and H. A. Scheraga, *J. Chem. Phys.*, **42**, 2209 (1965).

(17) E. Giglio, *Nature (London)*, **222**, 339 (1969).

(18) D. R. Herschbach in "International Symposium of Molecular Structural Spectroscopy," Butterworths, London, 1963.

(19) C. W. Bunn, *Proc. Roy. Soc., Ser. A*, **180**, 67 (1942); M. L. Huggins, *J. Chem. Phys.*, **13**, 37 (1945); L. Pauling, R. B. Corey, and H. R. Branson, *Proc. Nat. Acad. Sci. U. S. A.*, **37**, 205 (1951); G. Natta and P. Corradini, *Nuovo Cimento, Suppl.*, **15**, 9 (1960).

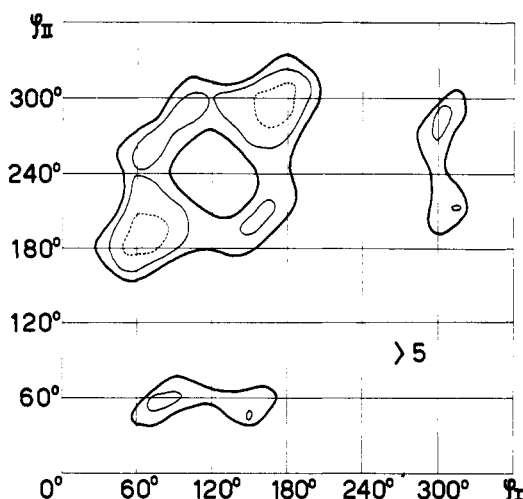


Figure 3. $E_h(\varphi_I, \varphi_{II})$ plot for the helical chain. Energy levels are drawn at 1 (dashed line), 3, 5 (heavy line) kcal/mol.

for the IPP chain in the crystalline state.²⁰ However, in addition to the two equivalent absolute minima approximately corresponding to the $\dots(\text{TG}')(\text{TG}')\dots$ and $\dots(\text{GT})(\text{GT})\dots$ threefold helices with opposite sense of spiralization (the pairs within parentheses refer to the odd-even sequence, see Figure 1), eight more minima appear in the map, equivalent in pairs, whose energy is less than 3 kcal/mol above the lowest minima. This represents a novel feature in comparison with energy maps obtained hitherto, and is strictly connected with the relatively low value of $r(\text{CH}_3)$ (1.8 Å). As an example, no other minimum obtained with $r(\text{CH}_3) = 2$ Å is characterized by an energy lower than 3.6 kcal/mol. The many low lying energy minima of Figure 3 clearly suggest that inversion of chain spiralization (*i.e.*, from the $\dots(\text{TG}')(\text{TG}')\dots$ to the $\dots(\text{GT})(\text{GT})\dots$ conformation, and *vice versa*) may take place with a relatively high probability.

Characteristic Ratio: Calculation According to the asr Scheme and Comparison with Experimental Data. The characteristic ratio C_∞ relative to the unperturbed mean-square length of the chain has been evaluated according to the equation recently proposed by some of us (see ref 11, eq 23)

$$C_\infty = \langle r^2 \rangle_0 / 2Nl_\infty^2 = (100) \mathbf{a}_3^* (\mathbf{E} + \Psi_{T1}) (\mathbf{E} + \mathbf{Z} \Psi_{T1})^{-1} (\mathbf{E} + \mathbf{Z}) \begin{pmatrix} 1 \\ 0 \\ 0 \end{pmatrix} \quad (3)$$

The matrices in the right-hand side are built up with the Fourier expansion coefficients of the statistical weights corresponding to both the odd-even and the even-odd energy plots, as well as with the elements of the 3×3 matrices which represent the rotation around each skeletal bond. The order of the square matrices \mathbf{E} (unit matrix), Ψ_{T1} and \mathbf{Z} is $3(2\bar{m} + 1)$, where \bar{m} is the highest index taken into consideration in the Fourier expansion of the statistical weight (*i.e.*, all the Fourier terms containing $\cos m\varphi$ or $\sin m\varphi$ with $m > \bar{m}$ are neglected). The conformational partition function is (see ref 11, eq 5)

$$\mathbf{Z} = (2\pi)^{2N} \lambda^N \quad (4)$$

where λ is the largest eigenvalue of an appropriate square matrix of order $(2\bar{m} + 1)$ built up with the Fourier coefficients.

(20) (a) P. Corradini, P. Ganis, and P. Oliverio, *Atti Accad. Naz. Lincei, Cl. Sci. Fis., Mat. Natur., Rend.*, **33**, 320 (1962); (b) P. de Santis, E. Giglio, A. M. Liquori, and A. Ripamonti, *J. Polym. Sci., Part A*, **1**, 1383 (1963).

Table II
Characteristic Ratios (C_∞) of IPP for Different $r(\text{CH}_3)$ Values (Å) Calculated with the asr Scheme for Both Sets of Non-bonded Interaction Parameters

$r(\text{CH}_3)$	Set I			Set II	
	100°	150°	200°	100°	200°
2.00	12.31		7.60	9.59	6.16
1.90	8.49		5.68	6.24	4.56
1.85	6.81	5.60	4.81		
1.80	5.43		4.10	4.31	3.60
1.70	3.41		2.99	3.11	2.93

Table III
Test of Convergence for λ and C_∞ on the Basis of the Parameters of Set I with $r(\text{CH}_3) = 1.85$ Å

\bar{m}	50°		100°		150°		200°	
	$\lambda \times 10^5$	C_∞	$\lambda \times 10^5$	C_∞	$\lambda \times 10^5$	C_∞	$\lambda \times 10^5$	C_∞
7	305	10.03	487	7.34	723	5.87	1017	4.98
10	317	8.67	500	6.77	737	5.58	1029	4.81
14	315	8.92	499	6.85	736	5.61	1029	4.82

Table IV
Temperature Coefficient $d \ln \langle r^2 \rangle_0 / dT$ ($\times 10^3$) in the 100–200° Range for Various $r(\text{CH}_3)$ Values (Å)

$r(\text{CH}_3)$	1.70	1.80	1.85	1.90	2.00
Set I	-1.29	-2.84	-3.48	-4.01	-5.09
Set II	-0.59	-1.81		-3.13	-4.43

Table V
Average Temperature Coefficients $d \ln \langle r^2 \rangle_0 / dT$ ($\times 10^3$) in Different Temperature Ranges ($r(\text{CH}_3) = 1.80$ Å for Both Sets)

Temp Range (°C)	Set I	Set II
50–100	-4.18	-3.12
100–150	-3.17	-2.10
150–200	-2.38	-1.50

The characteristic ratios obtained for all the non-bonded interaction parameters reported in Table I are given in Table II. It should be noticed that the corresponding results of C_∞ for the two sets of parameters never differ by more than 25% of their average value. The highest order \bar{m} considered in the Fourier expansion is 12 in all cases. This value was chosen after a test of the rate of convergence of the results with increasing \bar{m} . As it is shown in Table III for the specific case with $r(\text{CH}_3) = 1.85$ Å and set I of the parameters, both λ and C_∞ do not show significant changes for $\bar{m} > 10$, and substantially similar conclusions may be derived for all the other sets of parameters. The temperature coefficient of the characteristic ratio, $d \ln \langle r^2 \rangle_0 / dT$, deduced from the data reported in Table II and averaged over the range 100–200°, is shown in Table IV. From Table V it may be seen that the temperature derivative displays a decreasing trend in absolute value with increasing temperature, in agreement with experimental observation on both isotactic poly(*n*-pentene-1)²¹ and poly(*n*-butene-1).²²

(21) (a) G. Moraglio and G. Gianotti, *Eur. Polym. J.*, **5**, 781 (1969); (b) G. Moraglio, G. Gianotti, and F. Zoppi, *Int. Symp. Macromol., Leiden*, 1970, Abstr. 146.

(22) G. Moraglio, G. Gianotti, F. Zoppi, and U. Bonicelli, *Eur. Polym. J.*, **7**, 303 (1971).

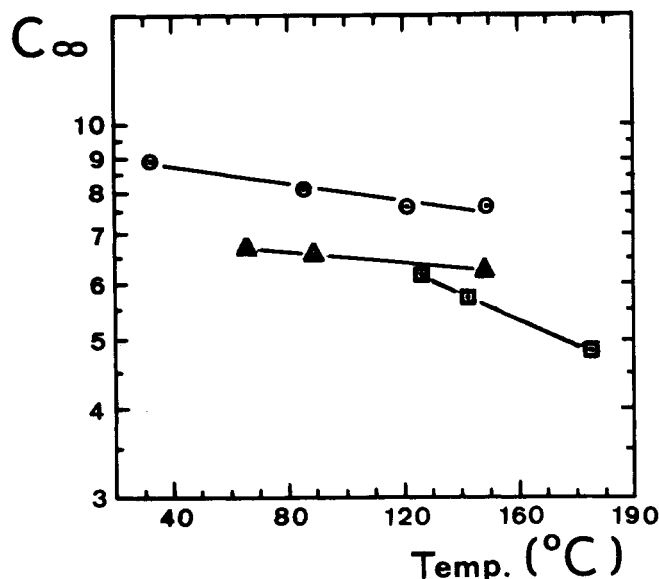


Figure 4. Semilogarithmic plot of the experimental characteristic ratios C_∞ vs. T ($^{\circ}\text{C}$) for isotactic poly(*n*-pentene-1) (O), poly(*n*-butene-1) (Δ), and poly(propylene) (\square). The best-fitting straight lines have been drawn.

The intrinsic viscosity measurements performed by Kinsinger and Hughes^{7b} in Θ solvents give $K = 13.2\text{--}11.2 \times 10^{-4} \text{ dl mol}^{1/2}/\text{g}^{3/2}$ between 145 and 153 $^{\circ}$, where

$$K = [\eta]_0 M^{1/2} = \Phi \langle r^2 \rangle_0 / M^{3/2} \quad (5)$$

Taking the average values $K = 12 \times 10^{-4}$ and $T = 150^{\circ}$ and assuming $\Phi = 2.6 \times 10^{21}$ (ref 2, p 37), the characteristic ratio C_∞ is 5.29. From more recent data obtained in Θ solvents by Nakajima and Sayjio⁸ in the temperature range 120–180 $^{\circ}$, the value of C_∞ at 150 $^{\circ}$ is about 5.2 if $\Phi = 2.87 \times 10^{21}$; furthermore, they obtain $d \ln \langle r^2 \rangle_0 / dT = -4.1 \times 10^{-3}$. With $\Phi = 2.6 \times 10^{21}$, C_∞ becomes 5.55, still in good agreement with the results obtained by Kinsinger and Hughes.^{7b} All these values have been substantially confirmed by recent measurements in Θ solvents performed by one of us on IPP (G. M.⁹). From inspection of Table II we see that the best-fitting values of $r(\text{CH}_3)$ are close to 1.85 Å for set I and to 1.90 Å for set II, which give $C_\infty = 5.6$ and 5.2, respectively. The corresponding temperature derivatives are -3.5 and -3.1×10^{-3} , in good agreement with the experimental figure (see Table IV). The above values of $r(\text{CH}_3)$ are close to those which account for the gauche-trans energy difference of *n*-butane (1.75 and 1.80 Å for sets I and II, respectively) and the value corresponding to set I is not far from that chosen for poly(isobutylene) (1.70 Å).¹² Incidentally, we want to point out that set II seems to be a better representation of the non-bonded interactions involving the methyl group, inasmuch as it fits the experimental data with a van der Waals radius which is closer to that usually observed in crystals.

It is of interest to consider the experimental data in Θ solvents obtained by one of us for isotactic poly(*n*-pentene-1)²¹ and poly(*n*-butene-1)²² in the light of the present results.

Figure 4 shows the plot of the characteristic ratio C_∞ vs. T for these polymers derived from $[\eta]_0$ assuming $\Phi = 2.6 \times 10^{21}$ (see eq 5); the corresponding plot obtained with the same Φ from the experimental data of Nakajima and Sayjio⁸ is also given for IPP. At about 150 $^{\circ}$ the average chain extension decreases in the order: polypentene > polybutene > polypropylene, although for polypropylene it

shows the largest trend to increase with decreasing temperature. This sequential order is in qualitative agreement with the results reported in Table II, if the possibility of restricted rotation of the side groups around the C–C bonds is taken into account.^{21a} As a consequence, the effective average radius of the side group increases from polypropylene to polypentene, determining an increasing characteristic ratio, as it should be expected. The low value of the temperature derivative of polybutene and polypentene, in comparison with polypropylene, may be interpreted by considering that the relative rotational freedom of the side group is progressively hindered with decreasing temperature. At lower temperatures, these groups will tend to assume only those conformations which minimize the intra-chain repulsion, with the consequence that the effective average radius (in qualitative terms) decreases, and the characteristic ratio is lower than expected for a side group with a fixed size.

In contrast to the above results, force-temperature measurements performed by Mark and Flory yield a slightly positive value for the temperature coefficient of the characteristic ratio for both isotactic poly(*n*-butene-1) and poly(*n*-pentene-1).²³ However, we think it appropriate to rely upon the data obtained from Θ solutions only, in spite of the random errors that might be introduced by specific solvent-polymer interactions. The reason of our choice is essentially the following. We believe that the assumption of nearly unperturbed configurations for the polymer chains in the amorphous state, useful as it has proved to be for the basic development of the statistical theory of rubber,^{24,25} is probably too rough for a sort of a second-order perturbation effect, such as the temperature derivative of the characteristic ratio, to be derived correctly. Essentially, the effect of chain packing must lead to some deviations from the unperturbed behavior. Although we do not believe that these deviations significantly affect the conformations of relatively short chain segments, they might influence the average size of the chain as a whole.¹¹ As an example, the existence of relatively numerous folds in the amorphous polymer phase, which seems to be reasonably well proven,²⁶ should have some effect upon the mean-square end-to-end distance and, even more, upon its temperature coefficient. As a matter of fact, for several synthetic polymers the values of $d \ln \langle r^2 \rangle_0 / dT$ deduced by force-temperature measurements are systematically shifted toward the positive side with respect to those derived from Θ solutions (see ref 27 and ref 8 and 9 in that reference).

Characteristic Ratio Calculated According to the ris Scheme. We will show in the following some calculations of C_∞ according to the ris approximation. It is important to stress that we were not interested in any accurate investigation in this direction, being concerned primarily with a rough comparison between the two methods, once the same energy maps are used as the starting point. Consequently, we did not go further than selecting five isomeric states per each rotation angle, which are shown in Table VI, together with the energies of all their combinations in neighboring pairs, for the particular case of set I, $r(\text{CH}_3) = 1.85$ Å (see Table I for the energy parameters). We have employed an analytical expression of C_∞ formally identical with eq 3 except for a different meaning of

(23) J. E. Mark and P. J. Flory, *J. Amer. Chem. Soc.*, **87**, 1423 (1965).

(24) P. J. Flory, *Chem. Rev.*, **35**, 51 (1944); F. T. Wall, *J. Chem. Phys.*, **10**, 485 (1942).

(25) P. J. Flory, "Principles of Polymer Chemistry," Cornell Univ. Press, Ithaca, N. Y., 1953, Chapter XI.

(26) G. S. Y. Yeh, *J. Macromol. Sci.*, **B6**, 465 (1972).

(27) G. Allegra, *Makromol. Chem.*, **110**, 58 (1967).

Table VI
Energies (kcal/mole) for the Rotational Isomeric Pairs of the Odd-Even and Even-Odd Type Obtained with the Parameters of Set I ($r(\text{CH}_3) = 1.85 \text{ \AA}$)

φ_{2i-1}	φ_{2i}					φ_{2i}	φ_{2i+1}				
	55	190	210	270	300		60	90	150	170	305
60	5.0	0.4	0.2	2.7	36.0	55	1.5	2.0	1.1	1.2	100.0
90	3.2	2.9	2.0	2.5	4.8	190	1.0	0.9	1.0	1.1	0.9
150	3.8	4.5	2.6	2.1	2.4	210	2.6	2.2	2.7	2.4	2.3
170	9.0	20.0	3.0	1.5	1.2	270	4.8	2.5	2.1	2.1	3.1
305	100.0	10.0	2.6	2.3	8.0	300	36.0	2.6	0.3	0.2	0.5

Table VII
Characteristic Ratios (C_∞) of IPP for Different $r(\text{CH}_3)$ Values (\AA) Calculated with the ris Scheme for both Sets of Non-bonded Interaction Parameters

$r(\text{CH}_3)$	Set I		Set II	
	100°	200°	100°	200°
2.00	27.0	11.2	16.8	8.0
1.90	18.7	9.8	8.8	5.7
1.85	12.6	7.2		
1.80	10.6	7.1	5.9	4.3
1.70	4.6	3.5		

the matrices;¹¹ this expression is equivalent to that formerly proposed by Hoeve.²⁸ The results are shown in Table VII for all the different sets of parameters and for the two temperatures of 100 and 200°. They are always larger than the corresponding results obtained with the asr scheme, the percentage difference decreasing with either smaller values of $r(\text{CH}_3)$ or higher temperatures. We believe the reason of this discrepancy is essentially twofold. First, we did not try to optimize the energy associated with each pair ($\varphi_i\varphi_{i+1}$) by inspecting composite energy maps involving φ_{i+2} and/or φ_{i-1} as well (cf. the considerations reported earlier). Instead, the five isomeric states for each rotation angle were derived from the energy plot of the helical chain (see Figure 3). With reference to the energy values reported in Table VI for set I, $r(\text{CH}_3) = 1.85 \text{ \AA}$, it is possible to verify that, while the helix inversion $(\dots\text{T})(\text{GT})(\text{TG})(\text{T}\dots)$ (even-odd pairs in parentheses) is possible with no extra energy over that of the helical sequences $(\dots\text{T})(\text{GT})(\text{GT})(\text{G}\dots)$ and $(\dots\text{G}')(\text{TG})(\text{TG})(\text{T}\dots)$, the opposite inversion may take place with any of the following sequences: $(\dots\text{G}')(\text{TG})(\text{T}-\text{T})(\text{G}\dots)$ or its equivalent $(\dots\text{G}')(\text{TT})(\text{GT})(\text{G}\dots)$, and $(\dots\text{G}')(\text{TG})(\text{G}'\text{T})(\text{G}\dots)$, or its equivalent $(\dots\text{G}')(\text{T}-\text{G})(\text{GT})(\text{G}\dots)$, all of which involve an extra energy of about 4 kcal/mol. But—and now we come at the second reason of the discrepancy—there are many more conformations allowing the latter type of helix inversion with about the same extra energy or even less. As Corradini, Ganis, and Oliverio first pointed out,^{20a} these conformations are distributed within continuous ranges two of which, e.g., are: $\dots(\text{T}, \text{G}' - \alpha)(\text{G} + 60^\circ - \alpha, \text{T})\dots$ and $\dots(\text{T}, \text{G}')(\text{G} + 60^\circ + \alpha, \text{T} + \alpha)(\text{G}\dots)$, with $0 \leq \alpha \leq 60^\circ$. The lowest extra energy obtained for these conformations was 2.7 kcal/mole.^{4,20a} This is an interesting example of local conformational minima where the value of one rotation angle is influenced by that of a first neighbor. We believe it important to stress that, while this type of correlation is automatically accounted for in the asr scheme, it would require the artificial introduction of a few more rotational isomers per each skeletal bond within the ris scheme. Obviously, the neglect of these strained

Table VIII
 E^{conf}/N (kcal/mole) Calculated with Both Sets of the Non-bonded Interaction Parameters (asr Scheme)

T (°C)	Set I ($r(\text{CH}_3) = 1.85 \text{ \AA}$)	Set II ($r(\text{CH}_3) = 1.90 \text{ \AA}$)
50–100	0.85	0.96
100–150	1.07	1.20
150–200	1.30	1.42

conformations must lead to a value of C_∞ higher than expected, since it favors perpetuation of the regular $\dots(\text{TG}')(\text{TG}')\dots$ and $\dots(\text{GT})(\text{GT})\dots$ helices.⁴

Conformational Energy of Free IPP Chains. In the previous papers^{10,11} we have shown that the conformational energy per monomer unit is given by

$$E^{\text{conf}}/N = RT^2 d \ln \lambda / dT \quad (6)$$

the equation applying both to the asr and to the ris scheme. In the latter case λ is the largest eigenvalue of the matrix containing the statistical weights of the rotational isomers of the monomer unit, instead of the Fourier coefficients considered in the asr scheme (see eq 4). We have taken the zero value of the conformational energy corresponding to the regular threefold helices with the lowest energy. The results obtained from eq 6 at the melting temperature $T_M = 178^\circ$ within the asr scheme are 1.30 kcal/mol for set I, $r(\text{CH}_3) = 1.85 \text{ \AA}$, and 1.42 kcal/mol for set II, $r(\text{CH}_3) = 1.80 \text{ \AA}$, adopting the best-fitting values of $r(\text{CH}_3)$ (see Table VIII). Correcting the figures for the potential energy of oscillation around the bonds in the crystal at the melting temperature ($2 \times \frac{1}{2}RT$),¹¹ the intramolecular contribution to the heat of melting is 0.41 and 0.53 kcal per mol in the two cases. Values not very different are obtained from the ris scheme. The experimental value of ΔH_M is about 2.4 kcal/mol,²⁹ which means that the calculated intramolecular contribution accounts for about 20% of the total amount, i.e., a percentage slightly larger than in the case of poly(oxymethylene) but smaller than for polyethylene, where it is around 35–40%.¹¹

Final Comments. We have shown that the unperturbed dimensions of IPP may be accounted for theoretically by selecting proper sets of non-bonded interaction parameters which agree with formerly proposed data.^{11,12,17} The parameters chosen for the methyl...methyl interactions are close to the values producing the experimental gauche-trans energy difference of *n*-butane (0.8 kcal/mol¹⁴). The whole spectrum of skeletal rotations has been accounted for (asr scheme). The main advantage of this procedure is that all the important chain conformations allowing inversion between the $\dots(\text{TG}')(\text{TG}')\dots$ and the $\dots(\text{GT})(\text{GT})\dots$ threefold helices with opposite

(28) C. A. J. Hoeve, *J. Chem. Phys.*, **32**, 888 (1960).

(29) I. Kirshenbaum, Z. W. Wilchinsky, and B. Groten, *J. Appl. Polym. Sci.*, **8**, 2723 (1964).

handedness are taken into account, with a corresponding reduction in the characteristic ratio towards the experimental values. The same result is obtained by Boyd and Breitling within the ris scheme by (i) minimizing the energy of the local conformations by allowing several parameters to participate, and (ii) assuming a relative large number (i.e., 7) of rotational isomers per each skeletal bond.³ Since our treatment does not involve energy minimization, the energies corresponding to the different conformations are larger in our case than in Boyd and Brei-

ting's. Had the minimization process been carried out by us as well, it seems plausible that both the calculated characteristic ratio and the absolute value of its temperature coefficient would have even lower values.

We believe that both Boyd and Breitling's results and ours make any hypothesis about the presence of significant amounts of steric inversion in IPP⁶ unnecessary.

Acknowledgments. The authors acknowledge the support received by the Consiglio Nazionale delle Ricerche, Settore Chimico.

Form Factor of an Infinite Kratky-Porod Chain

J. des Cloizeaux

Service de Physique Théorique, Centre d'Etudes Nucléaires de Saclay,
91190 Gif-sur-Yvette, France. Received January 23, 1973

ABSTRACT: The form factor of an infinite Kratky-Porod chain of persistence length b can be defined by $bS(bq) = \int_{-\infty}^{+\infty} \langle \exp[iq \cdot \mathbf{r}(L)] \rangle dL$; $\mathbf{r}(L)$ represents the position of a point of the chain, where $S(p)$ is a universal function which is studied here. Analytic properties and precise values of this function are given.

The intensity of radiation scattered by an isolated chain molecule (for instance a dilute solution) is proportional to the form factor

$$S(\mathbf{q}) = \langle \sum_{ij} \exp[iq(\mathbf{r}_i - \mathbf{r}_j)] \rangle \quad (1.1)$$

Here the angular brackets indicate that $S(\mathbf{q})$ is obtained by averaging over all chain configurations and \mathbf{q} is the momentum transfer.

For small-angle X-ray scattering of long molecules, it is tempting to use for comparison with experiments, a simplified model, the well-known Kratky-Porod chain.¹⁻⁷

For an infinite Kratky-Porod chain of persistence length b , the form factor can be defined by

$$s_{\infty}(\mathbf{q}) = \int_{-\infty}^{+\infty} dL \langle \exp[iq \cdot \mathbf{r}(L) - \mathbf{r}(0)] \rangle \quad (1.2)$$

Here $\mathbf{r}(L)$ indicates the position of a point on the chain and L the length measured along the chain (see Figure 1). The derivative of $\mathbf{r}(L)$ with respect to L is a unit vector $\dot{\mathbf{r}}(L)$ ($|\dot{\mathbf{r}}(L)| = 1$) which is tangent to the curve and we recall that b is defined by

$$\cos \alpha_{12} = \langle \dot{\mathbf{r}}(L_1) \cdot \dot{\mathbf{r}}(L_2) \rangle = \exp[-|L_1 - L_2|/b] \quad (1.3)$$

where α_{12} is the angle between the chain directions in positions L_1 and L_2 . For $L \gg b$, we have also

$$\langle [\mathbf{r}(L) - \mathbf{r}(0)]^2 \rangle \approx 2Lb$$

which is a consequence of eq 1.3.

Introducing dimensionless quantities, we see immediately that

where $S(p)$ is a universal function which we plan to study here. Actually, it is the form factor of a Kratky-Porod chain of unit persistence length. Therefore, in the following, we shall consider only such chains.

Basic Equations

It is convenient to introduce the auxiliary function $F(\mathbf{p}, \mathbf{t}; L)$ which is the expectation value of $\exp[i\mathbf{p} \cdot \mathbf{r}(L) - \mathbf{r}(0)]$ for chains of length L , starting in a given direction \mathbf{t} , i.e., such that $\dot{\mathbf{r}}(0) = \mathbf{t}$ (with $|\mathbf{t}| = 1$ for any L). More explicitly

$$F(\mathbf{p}, \mathbf{t}; L) = \langle \delta_s[\dot{\mathbf{r}}(0) - \mathbf{t}] \exp[i\mathbf{p} \cdot \mathbf{r}(L) - \mathbf{r}(0)] \rangle \quad (2.1)$$

where δ_s is a surface Dirac function.

Thus

$$S(p) = \int_{-\infty}^{+\infty} dL \int d\Omega(\mathbf{t}) F(\mathbf{p}, \mathbf{t}; L) \quad (2.2)$$

It is also convenient to set

$$\mathbf{p} \cdot \mathbf{t} = p \cos \theta \quad (2.3)$$

and with this notation

$$d\Omega(\mathbf{t}) = 2\pi \sin \theta d\theta \quad (2.4)$$

For obvious symmetry reasons

$$F(-\mathbf{p}, -\mathbf{t}; L) = F(-\mathbf{p}, \mathbf{t}; -L) = F(\mathbf{p}, \mathbf{t}; L) \quad (2.5)$$

and therefore, we may write as well

$$F(\mathbf{p}, \mathbf{t}; L) = \langle \delta_s[\dot{\mathbf{r}}(L) - \mathbf{t}] \exp[i\mathbf{p} \cdot \mathbf{r}(L) - \mathbf{r}(0)] \rangle \quad (2.6)$$

From this definition, we deduce an equation⁸ which determines $F(\mathbf{q}, \mathbf{t}; L)$ for $L > 0$

$$\frac{\partial}{\partial L} F(\mathbf{p}, \mathbf{t}; L) = \left[i\mathbf{p} \cdot \mathbf{t} + \frac{1}{2} \Delta_s \right] F(\mathbf{p}, \mathbf{t}; L) \quad (2.7)$$

(8) This equation is derived by using the fact that the motion of the extremity of $\mathbf{t}(L) \equiv \dot{\mathbf{r}}(L)$ on the unit sphere is Brownian. For chains defined by functional integrals, equations which resembles eq 2.7 have been derived by S. F. Edwards [*Disc. Faraday Soc.*, 49 (1970)] and K. S. Freed [*Advan. Chem. Phys.*, 22, 1 (1970)]. The difference comes from the fact that the Kratky-Porod chain is not Gaussian (with correlations) as those chains.

- (1) G. Porod, *J. Polym. Sci.*, 10, 157 (1953).
- (2) A. Peterlin, *J. Polym. Sci.*, 47, 403 (1960).
- (3) S. Heine, O. Kratky, G. Porod, and J. P. Schmitz, *Makromol. Chem.*, 44, 682 (1961).
- (4) N. Saito, K. Takahashi, and Y. Yunoki, *J. Phys. Soc. Jap.*, 22, 219 (1967); W. Gobush, H. Yamakawa, W. Stockmayer and W. S. Magee, *J. Chem. Phys.* 57, 2839 (1972).
- (5) Y. Fujiwara and P. J. Flory, *Macromolecules*, 3, 289 (1970).
- (6) H. E. Daniels, *Proc. Roy. Soc. Edinburgh, Sect. B*, 34, 63 (1951).
- (7) J. J. Hermans and R. Ullman, *Physica*, 18 (1952). The author is indebted to Dr. Ullman for bringing this and the previous article to his attention.